Research Square

Preprints are preliminary reports that have not undergone peer review.
They should not be considered conclusive, used to inform clinical practice,
or referenced by the media as validated information.

Motor-network changes following 10-Hz double-cone coil rTMS over the ipsilesional leg motor cortex in subacute stroke: a sham-controlled study using static and dynamic resting-state fMRI

Bin Su
Jiangsu Medical College
Zhipeng Pan
Shandong University of Traditional Chinese Medicine
Guilan Huang
Wuxi Central Rehabilitation Hospital
Yao Qian
Wuxi Central Rehabilitation Hospital
Xia Lu
Wuxi Central Rehabilitation Hospital
Yue Sun
Shandong University of Traditional Chinese Medicine
Hongrui Liu
Shandong University of Traditional Chinese Medicine
Xinran Ji
Shandong University of Traditional Chinese Medicine
Boyuan Zhu
Changzhi Medical College
Qiguang Li
Fudan University
Xiangtong Ji
Fudan University
Limin Sun
tracy611@sina.com

Fudan University
Jianxia Lu
111164@jsmc.edu.cn

Jiangsu Medical College
Hewei Wang
wanghew@fudan.edu.cn

Fudan University

Research Article

Keywords: stroke, lower-limb motor recovery, repetitive transcranial magnetic stimulation, double-cone coil, resting-state functional MRI, functional connectivity, cerebellum

Posted Date: November 22nd, 2026

DOI: https://doi.org/10.21203/rs.3.rs-11787392/v1

License: This work is licensed under a Creative Commons Attribution 4.0 International License. Read Full License

Additional Declarations: The authors declare no competing interests.

Abstract

Background: High-frequency repetitive transcranial magnetic stimulation (rTMS) targeting the leg motor cortex can improve lower-limb function after stroke, but its effects on distributed motor networks remain unclear.

Methods: In a randomized, double-blind, sham-controlled study, 32 patients with subacute stroke received 15 sessions of 10-Hz double-cone coil rTMS over the ipsilesional leg motor cortex or sham over 3 weeks alongside conventional rehabilitation. The Fugl–Meyer Assessment of the Lower Extremity (FMA-LE) and resting-state fMRI were obtained before and after treatment. Analyses included 31 patients (12 rTMS, 19 sham). Static and dynamic fractional amplitude of low-frequency fluctuations (fALFF) and leg motor seed-based functional connectivity (FC) were assessed across cortical motor and somatosensory, basal ganglia, and cerebellar regions. Spearman correlations examined associations with FMA-LE improvement.

Results: FMA-LE improvement was greater with rTMS than sham (difference, 5.246 points; 95% CI, 2.728–7.764; $P < 0.001$). Relative to sham, the rTMS group showed increased fALFF in ipsilesional presupplementary motor and premotor cortices and decreased fALFF in contralesional sensorimotor cortex and cerebellar lobule VIII. Leg motor seed FC showed greater increases with supplementary motor and cerebellar–vermian IV/V regions and a greater decrease with the ipsilesional caudate. The rTMS group also showed greater reductions in contralesional sensorimotor and cerebellar Crus I/VI fALFF variability and ipsilesional cerebellar Crus I/II FC variability. Correlation analyses linked greater FMA-LE improvement to larger reductions in sensorimotor fALFF variability ($\rho = -0.649$, $P < 0.001$) and lobule VIII fALFF ($\rho = -0.566$, $P < 0.001$), and larger increases in leg motor seed FC with the cerebellar–vermian region ($\rho = 0.502$, $P = 0.004$).

Conclusions: 10-Hz double-cone coil rTMS improved lower-limb motor function compared with sham and was accompanied by distributed functional changes across cortical, striatal, and cerebellar regions. Cerebellar functional reorganization may contribute to the motor benefits of leg motor cortex stimulation.

Trial registration: Chinese Clinical Trial Registry, ChiCTR2000041231; registered 22 December 2020.

Background

Lower-limb recovery after stroke requires more than the return of isolated muscle strength. Standing, transferring, and walking depend on coordinating voluntary movement with postural adjustments and sensory feedback [1, 2]. These demands engage cortical motor and sensory areas together with subcortical and cerebellar circuits. Task-fMRI studies of lower-limb movement after stroke have reported altered interhemispheric coupling and sensorimotor–cerebellar connectivity [3, 4]. Understanding how this distributed system responds to rehabilitation could help explain the brain changes accompanying gains in lower-limb motor control.

Repetitive transcranial magnetic stimulation (rTMS) is used as an adjunct to rehabilitation to modify motor-system excitability [5]. Meta-analyses report benefits for lower-limb function and mobility, although outcomes vary with the stimulation protocol and clinical measure [6, 7]. The medial location of the leg motor representation makes it less accessible to conventional figure-of-eight stimulation; a double-cone coil reaches deeper tissue with a broader induced field [8]. An early crossover study reported walking improvements after high-frequency double-cone stimulation [9]. Our previous randomized, double-blind trial in an independent cohort also showed greater improvements in lower-limb motor function and balance with 10-Hz double-cone rTMS than with sham stimulation [10]. Despite these clinical benefits, how this stimulation regimen affects the broader motor network remains unclear.

Neuroimaging studies link walking improvements after lower-limb rehabilitation to changes in sensorimotor, cingulate motor, striatal, and cerebellar activity [11, 12]. Lower-limb mirror therapy has been associated with altered spontaneous activity and functional connectivity [13], while robot-assisted gait training has linked walking gains to changes in whole-brain network efficiency and clustering [14]. Connectivity–behavior relationships vary by circuit: greater long-range connectivity density in bilateral supplementary motor area (SMA) was associated with better lower-limb function [15], whereas stronger ipsilesional SMA–premotor connectivity was associated with poorer walking balance [16]. In chronic stroke, stronger SMA and premotor connections to contralateral motor and thalamic regions were related to better gait coordination and mobility [17]. Beyond cortical and thalamic motor circuits, intervention studies also support cerebellar involvement in lower-limb recovery. In a sham-controlled trial, cerebellar stimulation improved balance and reduced step width alongside increased posterior parietal responses measured using transcranial magnetic stimulation and electroencephalography [18]. A recent vermis-stimulation trial linked balance gains to stronger connectivity between vermis X and bilateral occipitotemporal cortices [19]. Physiological studies link the SMA to anticipatory postural adjustments and the cerebellum to coordinating these adjustments with stepping [20]. Primate tracing identifies cerebellar outputs to the SMA and pre-supplementary motor area (preSMA) [21]. Together, these findings provide a rationale for examining cortical and cerebellar responses to leg motor cortex stimulation in relation to lower-limb motor recovery.

Resting-state fMRI examines spontaneous brain activity and connectivity without requiring standardized movement in the scanner, making it suitable for patients with motor impairment [22]. Longitudinal resting-state studies have linked changes in motor-network connectivity to stroke recovery [23]. Fractional amplitude of low-frequency fluctuations (fALFF) characterizes regional low-frequency BOLD fluctuations, while seed-based functional connectivity (FC) measures temporal coupling between regions [24, 25]. These measures are typically summarized over the full scan, although regional activity and connectivity fluctuate over time [26]. Dynamic analyses characterize this temporal variability, which may reveal features of motor dysfunction and recovery beyond scan-averaged measures [27]. We therefore examined both static and dynamic measures to characterize regional activity, connectivity, and their temporal variability following stimulation.

In this randomized, sham-controlled study, we investigated brain functional changes following 3 weeks of 10-Hz double-cone coil rTMS over the ipsilesional leg motor cortex, with both groups receiving conventional rehabilitation. Using static and dynamic resting-state fMRI, we characterized regional activity, functional connectivity, and their temporal variability within the motor network. We aimed to determine whether these measures changed differently between rTMS and sham and whether their changes were associated with improvements in lower-limb motor function.

Methods

Study design and participants

The study design and resting-state fMRI analysis framework are summarized in Fig. 1. This randomized, sham-controlled study enrolled 32 participants at Wuxi Tongren Rehabilitation Hospital between January 2021 and March 2022. The study was approved by the Institutional Review Board of Wuxi Mental Health Center (approval no. WXMHCIRB2020LLky013; July 29, 2020) and prospectively registered with the Chinese Clinical Trial Registry (ChiCTR2000041231; December 22, 2020). Written informed consent was obtained from all participants.

The protocol specified the following inclusion criteria: (1) stroke diagnosed according to the diagnostic criteria adopted at the Fourth National Conference on Cerebrovascular Diseases and confirmed by CT or MRI; (2) age 40–70

years; (3) a clinically stable condition within 6 months of stroke onset; (4) first-ever stroke with unilateral hemiplegia and lower-limb motor impairment; (5) Brunnstrom stage II or higher for the affected lower limb; (6) right-handedness; (7) absence of aphasia and ability to communicate effectively; (8) a Mini-Mental State Examination score of at least 24 [28]; and (9) agreement to participate by the patient and family, with written informed consent obtained. The exclusion criteria were: (1) a cardiac pacemaker or metallic implant; (2) severe bone, joint, or muscle disease; (3) severe hepatic, renal, or other life-threatening disease, or a psychotic disorder; (4) a personal or family history of epilepsy; (5) a skull defect; (6) extensive cerebral infarction or intracerebral hemorrhage; (7) unwillingness to receive the study intervention; or (8) concurrent participation in another clinical trial. Device-related contraindications and seizure risk were considered in accordance with expert TMS safety recommendations [29].

After baseline assessment, an independent physician allocated participants to rTMS or sham stimulation using a computer-generated random sequence. Group assignments were concealed in opaque, sealed envelopes. A research coordinator provided the assigned active or sham coil. The active and sham coils were identical in appearance, with identifying information concealed. Participants, stimulation therapists, and outcome assessors were blinded to group assignment, following the procedures described in our separate clinical trial [10]. The stimulation operator was not involved in outcome assessment. Recruitment was interrupted by COVID-19-related disruptions after 32 of the planned 64 participants had been enrolled, and subsequent review of clinical outcomes informed the decision not to resume recruitment. Further details are provided in the Supplementary Methods.

Intervention

Participants received rTMS or sham stimulation according to the same protocol used in our separately conducted randomized controlled trial [10]. The intervention comprised 15 sessions over 3 weeks, delivered 5 days per week. Both groups also received conventional rehabilitation, including lower-limb strengthening, trunk control exercises, sit-to-stand practice, balance exercises, and gait training, tailored to each participant's functional ability.

rTMS was delivered using a Magneuro100 stimulator (Nanjing VISHEE Medical Technology Co., Ltd., China) equipped with a double-cone coil (VCZ001). Stimulation targeted the ipsilesional leg motor hotspot, identified by motor-evoked potentials recorded from the paretic tibialis anterior muscle. Resting motor threshold was defined as the lowest stimulation intensity that elicited responses exceeding 50 μV in at least 5 of 10 trials [30]. When MEPs could not be elicited from the paretic tibialis anterior, the hotspot for the nonparetic tibialis anterior was identified in the contralesional hemisphere, and its mirror location across the midline was used as the ipsilesional stimulation site. In these participants, stimulation intensity was set at 90% of the contralesional resting motor threshold. Each session consisted of 24 trains of 50 pulses delivered at 10 Hz and 90% of resting motor threshold, with 47-s intervals between trains, yielding 1,200 pulses per session. Sham stimulation used a dedicated sham coil placed over the same ipsilesional target, with the same session schedule and train timing. The sham coil was identical in appearance to the active coil and produced a similar acoustic output.

Clinical assessment

Lower-limb motor function was assessed at baseline and after the 3-week intervention using the Fugl–Meyer Assessment of the Lower Extremity (FMA-LE) [31, 32]. Scores range from 0 to 34, with higher scores indicating better motor function. Change in FMA-LE score was calculated as the postintervention score minus the baseline score.

MRI acquisition and preprocessing

At baseline and after the intervention, structural and resting-state functional MRI scans were acquired within 24 h of the corresponding clinical assessment using a 3.0-T Siemens Skyra scanner (Siemens, Germany). T1-weighted images were acquired using a three-dimensional magnetization-prepared rapid acquisition gradient-echo sequence with a repetition time (TR) of 2530 ms, an echo time (TE) of 2.34 ms, an inversion time of 1100 ms, a flip angle of 7°, and 1-mm isotropic resolution. T2-weighted images were acquired using a three-dimensional SPACE sequence with TR/TE = 3000/298 ms and approximately 0.9-mm isotropic resolution. Resting-state functional images were acquired using gradient-echo echo-planar imaging with TR = 2030–2150 ms, TE = 30 ms, a flip angle of 90°, a field of view of 230 × 230 mm², a 64 × 64 acquisition matrix, 33–35 axial slices per volume, a slice thickness of 3.5 mm, an interslice gap of 0.875 mm, and 210 volumes per run.

Resting-state fMRI data were preprocessed using DPABI/DPARSF [33, 34]. The first 5 volumes were discarded, after which the remaining images underwent slice-timing correction and realignment. Participants whose head motion exceeded 2 mm of translation or 2° of rotation in any direction were excluded. T1-weighted images were reoriented, brain-extracted, and segmented into gray matter, white matter, and cerebrospinal fluid using New Segment. Functional images were normalized to Montreal Neurological Institute (MNI) space using DARTEL, resampled to 3-mm isotropic voxels, and spatially smoothed with a 4-mm full-width-at-half-maximum Gaussian kernel. Nuisance regression included a first-order polynomial trend, Friston's 24-parameter head-motion model, and white-matter, cerebrospinal-fluid, and global signals. For seed-based functional connectivity analyses, the time series were band-pass filtered at 0.01–0.10 Hz. To standardize lesion laterality for group-level analyses, images from participants with left-sided cerebral lesions were flipped along the left–right axis so that the ipsilesional hemisphere was represented on the right. Ipsilesional and contralesional labels referred to the side of the cerebral lesion, with the same spatial convention applied to cerebellar regions; the vermis was described as a midline structure.

Static and dynamic imaging measures

Regional spontaneous activity was quantified using the fractional amplitude of low-frequency fluctuations (fALFF) [24]. For each voxel, fALFF was calculated as the summed amplitude within the 0.01–0.08-Hz band divided by the summed amplitude across the full analyzed frequency range. The resulting maps were z-standardized before group-level analysis.

Seed-based functional connectivity (FC) was calculated using a spherical region of interest with a radius of 6 mm centered at MNI coordinates (6, − 30, 72), representing the ipsilesional leg motor region after laterality alignment. The seed location was informed by previous lower-limb functional imaging research [3]. The mean BOLD time series within the seed was correlated with the time series of each voxel within the search mask, and the resulting correlation coefficients were Fisher r-to-z transformed [25, 35].

All four static and dynamic measures were analyzed within the same motor-related search mask, comprising cortical motor and somatosensory regions from the Human Motor Area Template (HMAT) [36], basal ganglia regions from a basal ganglia template [37], and cerebellar and vermian regions from AAL3v1 [38]. The mask contained 16,972 voxels at 3-mm isotropic resolution. Its anatomical subdivisions are shown in Supplementary Fig. S1 and listed in Supplementary Table S1.

Dynamic fALFF and dynamic FC were estimated using a sliding-window approach [26], with a window length of 30 TR, a step size of 1 TR, and a Hamming window. Within each window, fALFF was recalculated in the 0.01–0.08-Hz

band, and FC was recalculated using the seed defined above. Temporal variability was quantified as the coefficient of variation (standard deviation divided by the mean) of window-specific fALFF values and the standard deviation of window-specific FC values. Window parameters and their conversion to seconds are described in the Supplementary Methods [39, 40].

Statistical analysis

Clinical analyses were performed using Python 3.12.14. Continuous variables are summarized as mean ± standard deviation, and categorical variables as counts. Change was defined as postintervention minus baseline. In participants with complete imaging data, FMA-LE changes were compared using an independent-samples Student's t test, reporting the unadjusted mean difference and 95% confidence interval.

Voxelwise imaging measures were analyzed using a 2 × 2 mixed-design analysis of variance, with group (rTMS and sham) as the between-subject factor and time (baseline and postintervention) as the within-subject factor. The group-by-time interaction was tested within the predefined motor-related search mask. Statistical significance was set at a voxel-level threshold of $P < 0.01$ and a cluster-level threshold of $P < 0.01$, with a minimum cluster size of 35 voxels. Regions selected by this analysis were summarized using group mean changes and descriptive independent-samples Student's t tests, with unadjusted mean differences and 95% confidence intervals [41]. Within each group, changes in the ten extracted imaging measures were also evaluated using two-sided paired t tests with 95% confidence intervals for mean changes. Unadjusted P values and Benjamini–Hochberg false discovery rate-adjusted P values across the 20 paired tests are provided in Supplementary Table S4.

Spearman rank correlations assessed associations between changes in static and dynamic imaging measures and FMA-LE improvement in the pooled sample and separately within the rTMS group. The association between changes in the two dynamic fALFF measures was examined in the pooled sample. Clinical comparisons and correlations were two-sided, with $P < 0.050$ used for these exploratory analyses; correlation P values were not adjusted across imaging measures. Exploratory mediation analyses examined indirect associations between FC changes and FMA-LE improvement (Supplementary Methods).

Results

Participants and lower-limb motor function

Of 135 participants assessed for eligibility, 32 were randomized to rTMS (n = 12) or sham stimulation (n = 20). One sham participant was excluded for excessive head motion, leaving 31 participants in the imaging analysis (12 rTMS and 19 sham; Supplementary Fig. S2). Participant characteristics and lesion distributions are presented in Table 1 and Fig. 2. FMA-LE scores increased in both groups over the 3-week intervention. Mean FMA-LE improvement was greater in the rTMS group than in sham (7.667 ± 3.229 vs. 2.421 ± 3.405 points), with an unadjusted between-group difference of 5.246 points (95% CI, 2.728–7.764; $P < 0.001$; Supplementary Fig. S3 and Table S2).

Table 1
Participant characteristics and lower-limb motor outcomes

Participant	Sex	Age (years)	Lesion site	Stroke type	Time since stroke (days)	Lesion side	Hemiparetic side	Baseline FMA-LE	Post-intervention FMA-LE
rTMS1	M	52	Med	I	20	L	R	12	24
rTMS2	M	51	BG, Med	I	27	L	R	27	31
rTMS3	M	62	BG, CR, Pons	I	54	L	R	12	21
rTMS4	M	63	BG, CR	I	83	R	L	16	28
rTMS5	M	57	BG, CR	I	65	L	R	15	22
rTMS6	M	65	BG, CR	I	55	R	L	14	23
rTMS7	M	65	CR, CSO	I	52	L	R	17	24
rTMS8	M	64	Pons	I	30	R	L	15	20
rTMS9	F	67	BG	I	30	R	L	15	20
rTMS10	M	66	CSO	H	123	L	R	12	23
rTMS11	M	63	CR	I	60	R	L	24	26
rTMS12	F	63	CR	I	73	L	R	13	22
Sham1	M	53	Tha, BG, CR	I	53	L	R	26	29
Sham2	F	65	CR	I	54	L	R	16	30
Sham3	M	69	BG, PVWM	I	120	L	R	18	25
Sham4	M	70	BG, CR	I	35	R	L	19	19
Sham5	M	70	BG	I	39	L	R	15	18
Sham6	M	52	BG, CR	I	45	L	R	10	16
Sham7	M	66	CR	I	45	L	R	14	16
Sham8	F	40	BG, CR	I	64	R	L	22	23
Sham9	M	53	BG	I	36	R	L	14	15
Sham10	F	58	BG, PVWM	I	65	R	L	21	21

M/F, male/female; I/H, ischemic/hemorrhagic stroke; L/R, left/right; BG, basal ganglia; CR, corona radiata; CSO, centrum semiovale; Tha, thalamus; Med, medulla oblongata; PVWM, periventricular white matter; CC, corpus callosum; FMA-LE, Fugl–Meyer Assessment of the Lower Extremity. Lesion and hemiparetic sides reflect original clinical records before image flipping.

Participant	Sex	Age (years)	Lesion site	Stroke type	Time since stroke (days)	Lesion side	Hemiparetic side	Baseline FMA-LE	Post-intervention FMA-LE
Sham11	M	61	Pons, BG	I	54	R	L	15	16
Sham12	M	55	BG	I	32	R	L	24	25
Sham13	M	63	BG, CR	I	74	L	R	21	22
Sham14	M	58	CR	I	120	R	L	22	22
Sham15	M	53	BG, CR	H	80	L	R	24	24
Sham16	M	58	CR	I	131	L	R	12	14
Sham17	M	64	BG	I	73	L	R	13	15
Sham18	F	70	CC (genu)	I	51	L	R	14	16
Sham19	M	63	BG, CR	I	38	L	R	16	16

M/F, male/female; I/H, ischemic/hemorrhagic stroke; L/R, left/right; BG, basal ganglia; CR, corona radiata; CSO, centrum semiovale; Tha, thalamus; Med, medulla oblongata; PVWM, periventricular white matter; CC, corpus callosum; FMA-LE, Fugl–Meyer Assessment of the Lower Extremity. Lesion and hemiparetic sides reflect original clinical records before image flipping.

Imaging findings

To examine brain changes accompanying lower-limb motor improvement, we analyzed static and dynamic resting-state fMRI. Group-by-time effects involved cortical, striatal, and cerebellar regions, with cortical and cerebellar changes associated with FMA-LE improvement (Figs. 3–5; Table 2). The anatomical composition of each region is detailed in Supplementary Table S3.

Table 2
Regional group-by-time effects on static and dynamic imaging measures

Measure	Region	Region voxels	Peak MNI x, y, z	Peak t
fALFF	I preSMA	40	3, 12, 48	3.962
fALFF	I premotor cortex (PMd/PMv)	38	48, 12, 42	4.048
fALFF	C sensorimotor cortex (S1/M1)	41	−63, − 15, 30	−3.912
fALFF	C cerebellum VIII	36	−15, − 63, −45	−4.687
FC	SMA/preSMA, predominantly C	63	−3, − 12, 60	3.412
FC	I caudate	42	9, 12, 6	−3.732
FC	Vermis and C cerebellum IV/V	39	−3, − 51, −3	6.051
dFALFF	C cerebellum Crus I/VI	55	−21, − 75, −27	−4.056
dFALFF	C sensorimotor cortex (S1/M1)	66	−54, − 27, 51	−5.476
dFC	I cerebellum Crus I/II	44	33, − 57, −39	−3.911

I/C, ipsilesional/contralesional relative to the cerebral lesion; the vermis is midline. MNI coordinates are in millimetres after lesion-side alignment. Voxel counts indicate extraction-region size. Peak t values represent (rTMS post − pre) − (sham post − pre), with 29 residual degrees of freedom. Anatomical subdivisions are detailed in Supplementary Table S3.

Changes in regional spontaneous activity

Group-by-time effects on z-standardized fALFF involved four cortical and cerebellar regions (Fig. 3A1–A4). Relative to sham, rTMS was associated with greater increases in predominantly ipsilesional pre-supplementary motor area (preSMA) and ipsilesional premotor cortex (PMd/PMv) fALFF. Between-group differences in change were 0.992 (95% CI, 0.578 to 1.405) for preSMA and 0.944 (95% CI, 0.603 to 1.285) for premotor cortex. Greater increases were associated with greater FMA-LE improvement in preSMA ($\rho = 0.473$, $P = 0.007$) and premotor cortex ($\rho = 0.390$, $P = 0.030$). Contralesional sensorimotor cortex (S1/M1) and cerebellar lobule VIII showed greater fALFF reductions with rTMS than sham, with between-group differences in change of − 0.926 (95% CI, − 1.362 to − 0.490) and − 0.786 (95% CI, − 1.133 to − 0.440), respectively. Greater reductions were associated with greater motor improvement in both regions (sensorimotor: $\rho = −0.383$, $P = 0.034$; lobule VIII: $\rho = −0.566$, $P < 0.001$; Fig. 5A). Paired tests supported the increases in preSMA and premotor cortex and decreases in sensorimotor cortex and lobule VIII within the rTMS group (all $P \leq 0.013$). In sham, changes reached significance in preSMA, premotor cortex, and lobule VIII (all $P \leq 0.033$), but not sensorimotor cortex ($P = 0.073$; Supplementary Table S4).

Changes in connectivity from the leg motor seed

Seed-based FC showed group-by-time effects in three regions (Fig. 3B1–B3). Relative to sham, rTMS was associated with greater increases in leg motor seed connectivity with bilateral SMA/preSMA, predominantly contralesional, and vermis/contralesional cerebellar lobules IV/V, and a more negative change in connectivity with the ipsilesional caudate (Supplementary Table S4). Within the rTMS group, SMA/preSMA and cerebellar–vermian FC increased; paired tests supported changes in these connections in both groups (all $P \leq 0.028$). Mean caudate FC shifted toward more negative values after rTMS (paired $P = 0.053$); the paired change in sham reached $P = 0.004$. These connections are summarized in Fig. 3B4. Greater increases in cerebellar–vermian FC were associated with

greater FMA-LE improvement (ρ = 0.502, P = 0.004; Fig. 5B). Pooled Spearman correlations with SMA/preSMA and caudate FC changes were not significant (P = 0.546 and 0.423, respectively; Supplementary Table S5).

An exploratory model linked changes in two connections from the leg motor seed to FMA-LE improvement: one with SMA/preSMA and the other with the vermis/contralesional cerebellar lobules IV/V. The model showed a positive indirect association through cerebellar connectivity change (standardized indirect effect, 0.802; 95% bootstrap CI, 0.525–1.167; Fig. 6). This indirect association remained positive after adjustment for treatment group (0.302; 95% bootstrap CI, 0.052–0.649) and in the rTMS group alone (0.637; 95% bootstrap CI, 0.189–1.734; Supplementary Fig. S4). In all three models, however, greater increases in SMA/preSMA connectivity were associated with less FMA-LE improvement when cerebellar connectivity change was held constant.

Changes in temporal variability of activity and connectivity

Three dynamic measures showed group-by-time effects, with greater reductions after rTMS than sham in contralesional sensorimotor and cerebellar Crus I/VI dFALFF variability and in leg motor seed connectivity variability with ipsilesional cerebellar Crus I/II (Fig. 4A–D). Between-group change comparisons yielded P < 0.001 for all three measures (Supplementary Table S4). All three measures decreased within the rTMS group; paired changes reached P < 0.010 in each group and remained significant after FDR correction (P < 0.05). dFALFF was expressed as a coefficient of variation and dFC as a standard deviation. The dynamic sensorimotor region predominantly involved S1, whereas the static region spanned S1/M1. Greater reductions in each dynamic measure were associated with greater FMA-LE improvement: sensorimotor dFALFF (ρ = −0.649, P < 0.001), cerebellar dFALFF (ρ = −0.446, P = 0.012; Fig. 5C), and cerebellar dFC (ρ = −0.453, P = 0.010; Fig. 5D). Sensorimotor dFALFF had the largest absolute correlation coefficient among the ten imaging measures. Sensorimotor and cerebellar dFALFF changes were also positively correlated (ρ = 0.737, P < 0.001; Supplementary Table S6): participants with larger sensorimotor reductions tended to show larger cerebellar reductions. Spearman correlations between imaging changes and FMA-LE improvement were assessed in the pooled sample (Supplementary Table S5).

Discussion

In this randomized, sham-controlled study, 10-Hz double-cone coil rTMS improved lower-limb motor function compared with sham and was accompanied by changes in resting-state brain function across the motor system. Static fALFF and seed-based FC analyses revealed changes in cortical, striatal, and cerebellar regions. Dynamic analyses further identified reduced temporal variability in sensorimotor and cerebellar regions. Several of these imaging changes were associated with FMA-LE improvement, suggesting that functional reorganization beyond the stimulated leg motor cortex may contribute to lower-limb motor recovery.

Cortical responses to leg motor stimulation

Following rTMS, fALFF increased in the ipsilesional preSMA and premotor cortex, accompanied by stronger connectivity between the leg motor seed and SMA/preSMA. These changes involved regions important for movement preparation and motor coordination. The double-cone coil can reach the medial leg motor representation, although its induced field is relatively broad, and TMS effects may extend to connected cortical regions [8, 42]. The SMA contributes to anticipatory postural adjustments during gait initiation [20], a function relevant to the balance and gait training undertaken during rehabilitation. Previous longitudinal imaging and stimulation studies have also associated motor recovery with changes in connected motor regions [43–45]. Increased fALFF in premotor areas

and stronger connectivity with medial motor regions may therefore reflect functional reorganization supporting lower-limb motor control.

Contralesional regions showed a different pattern: sensorimotor fALFF decreased, whereas connectivity between the leg motor seed and predominantly contralesional SMA/preSMA increased. This regional difference is consistent with evidence that contralesional contributions to stroke recovery vary with cortical location and structural reserve [46–49]. Enzinger et al. reported increased activation in bilateral sensorimotor cortex, cingulate motor areas, and the caudate during ankle movement after treadmill training [12]. Upper-limb studies have also reported reduced contralesional S1 task activation after motor imagery but increased contralesional M1 resting activity after mirror therapy [50, 51]. These varying findings may reflect differences in the interventions, cortical regions, and brain functions measured. In our pooled analyses, greater reductions in contralesional sensorimotor fALFF were associated with greater FMA-LE improvement, whereas changes in SMA/preSMA and caudate FC showed no significant individual correlations with improvement. The shift toward more negative caudate connectivity further suggests that the response extended into subcortical circuits within the interconnected cortical–basal ganglia–cerebellar system [52].

Cerebellar responses and temporal variability

Cerebellar changes were observed across several distinct regions. Following rTMS, fALFF decreased in contralesional lobule VIII, while connectivity between the leg motor seed and vermis/contralesional lobules IV/V increased. Both changes were associated with greater FMA-LE improvement. Lobules IV/V and VIII contain sensorimotor representations, whereas Crus regions participate in broader association networks [53–55]. Previous treadmill-training studies reported increased posterior cerebellar activation during movement, including contralesional Crus I, accompanying walking improvement [11]. Our findings complement these observations by showing changes in spontaneous activity and connectivity at rest. Evidence from motor learning, cerebellar stimulation, and studies of cerebellar pathway integrity and connectivity further supports cerebellar involvement in motor recovery [18, 56–58]. Recent studies of vermis stimulation [19] and multisensory BCI training [59] have also identified functional changes across distributed brain networks during rehabilitation.

The connectivity findings further suggest a relationship between cortical and cerebellar responses. In an exploratory model, increases in leg motor seed connectivity with SMA/preSMA were related to FMA-LE improvement through concurrent changes in seed connectivity with vermis/IV/V. Positive indirect associations were also observed after adjustment for treatment group and within the rTMS group. Although both connections originated from the leg motor seed, their relationship is consistent with the anatomical connections between cerebellar output and SMA/preSMA [21] and the complementary roles of these regions in postural preparation and stepping [20]. Previous research has similarly linked changes in SMA–cerebellar connectivity to balance improvement after SMA stimulation in stroke [60]. Interestingly, greater SMA/preSMA connectivity increases were associated with less motor improvement after accounting for cerebellar connectivity change. Such opposing direct and indirect associations can occur in statistical suppression models [61]. Peng et al. similarly found that stronger SMA–premotor connectivity was associated with poorer walking balance in chronic stroke [16]. In our study, the negative conditional association may reflect greater supplementary motor involvement in patients with continuing motor-control demands despite comparable changes in cerebellar connectivity.

Dynamic analyses provided additional information about the cerebellar and sensorimotor responses. Temporal variability decreased in contralesional sensorimotor cortex and cerebellar Crus I/VI, as well as in connectivity between the leg motor seed and ipsilesional cerebellar Crus I/II. Greater reductions in all three dynamic measures

were associated with greater FMA-LE improvement. Sensorimotor and cerebellar dFALFF changes were also strongly correlated across participants. Notably, the dynamic sensorimotor region predominantly involved S1, whereas the static region extended across S1/M1. Given the importance of sensory feedback in posture and locomotion, this finding raises the possibility that sensory-related functional changes accompany improvements in lower-limb motor control [2, 62]. Previous studies have linked time-varying network organization to motor impairment, recovery, and responses to rTMS [27, 63–65]. Our results extend these observations by identifying changes in both regional activity variability and connectivity variability after stimulation. Combining resting-state measures with sensory and locomotor assessments may help clarify how these changes relate to motor coordination during recovery [26, 66, 67].

Limitations

Several limitations should be considered. The relatively small sample and unequal group sizes limited the precision of treatment estimates and subgroup comparisons. Recruitment was interrupted by COVID-19 and was not resumed following review of the available clinical outcomes, which may have led to an overestimate of treatment benefit. Larger studies with longer follow-up and assessments of gait, balance, and mobility would help establish the durability and functional relevance of the observed improvements. Dynamic analyses used a single 30-TR window length, and testing alternative window lengths would help assess the consistency of these findings. As imaging was obtained only before and after treatment, we could identify changes in cortical and cerebellar connectivity but not determine whether they emerged simultaneously or at different stages of recovery. Additional imaging during rehabilitation could clarify the temporal development of these network changes.

Clinical implications and future directions

The distributed cortical and cerebellar responses observed after leg motor cortex stimulation suggest that treatment benefits may be influenced by the integrity and adaptability of the wider motor network. An important next step is to determine whether these network characteristics help explain individual responses to rTMS and how stimulation can be more effectively combined with task-specific rehabilitation. Longitudinal studies integrating functional imaging, structural motor-pathway measures, and assessments of gait, balance, and daily mobility could clarify whether treatment-related network changes predict longer-term functional outcomes and inform more individualized stimulation and rehabilitation strategies.

Conclusions

10-Hz double-cone coil rTMS targeting the ipsilesional leg motor cortex improved lower-limb motor function compared with sham in patients with subacute stroke. Treatment was accompanied by changes in regional activity and functional connectivity across cortical, striatal, and cerebellar regions, alongside reduced temporal variability in sensorimotor and cerebellar measures. Cerebellar changes in activity, connectivity, and temporal variability, together with reduced sensorimotor fALFF variability, were associated with motor improvement. These findings suggest that cortical–cerebellar functional reorganization may contribute to the motor benefits of leg motor cortex stimulation.

Abbreviations

BOLD	Blood-oxygen-level-dependent
CI	Confidence interval
CV	Coefficient of variation
DARTEL	Diffeomorphic Anatomical Registration Through Exponentiated Lie Algebra
dFALFF	Dynamic fractional amplitude of low-frequency fluctuations
dFC	Dynamic functional connectivity
DPABI	Data Processing & Analysis for (Resting-State) Brain Imaging
DPARSF	Data Processing Assistant for Resting-State fMRI
fALFF	Fractional amplitude of low-frequency fluctuations
FC	Functional connectivity
FDR	False discovery rate
FMA-LE	Fugl–Meyer Assessment of the Lower Extremity
fMRI	Functional magnetic resonance imaging
M1	Primary motor cortex
MEP	Motor-evoked potential
MNI	Montreal Neurological Institute
MRI	Magnetic resonance imaging
PMd	Dorsal premotor cortex
PMv	Ventral premotor cortex
preSMA	Pre-supplementary motor area
rTMS	Repetitive transcranial magnetic stimulation
S1	Primary somatosensory cortex
SD	Standard deviation
SMA	Supplementary motor area
TE	Echo time
TMS	Transcranial magnetic stimulation
TR	Repetition time

Declarations

Acknowledgements

We thank all participants for their time, cooperation, and contribution to this study. We also thank Kexu Zhang for assistance with data analysis, and Rui Zhang, Gufeng Li, Yefan Cao, Jianghua Liu, Canxin Zhou, and Xinna Tan for their contributions to data organization and lesion delineation.

Authors' contributions

Bin Su: Conceptualization, Investigation, Writing – Original Draft. Zhipeng Pan: Conceptualization, Formal analysis, Data curation, Writing – Original Draft. Guilan Huang, Yao Qian, Xia Lu: Investigation, Data collection. Yue Sun, Hongrui Liu, Xinran Ji, Qiguang Li, and Xiangtong Ji: Data curation, Validation. Boyuan Zhu: Methodology, Review & Editing. Limin Sun: Supervision, Writing – Review & Editing. Jianxia Lu and Hewei Wang: Supervision, Project administration, Writing – Review & Editing. All authors read and approved the final manuscript.

Funding

This work was supported by Jiangsu Medical College Research Start-up Funding Project (20256106), Key Medical Research Project of Jiangsu Commission of Health (K2025027), Yancheng Brain Health and Intelligent Rehabilitation Engineering and Technology Research Centre (YC2025609), China National Nature Science Young Foundation (82102665), Shanghai Sailing Program (21YF1404600), Jiangsu Medical College's Leading Talent Cultivation Support Program (000520240111), Rehabilitation Education Reform and Innovation Team Development Project (000520241028), the National Natural Science Foundation of China (81974356), Key Supporting Discipline Construction Project of Shanghai Health System (2023ZDFC0304), Shanghai Natural Science Foundation (23ZR1408500), Joint Foundation for Scientific and Technological Innovation of Fujian Province (2025Y9138), Natural Science Foundation of Fujian Province (2025J01724).

Data availability

The study's supporting data are available from the corresponding author upon reasonable request, subject to ethical and institutional restrictions on participant privacy protection.

Ethics approval and consent to participate

The study was approved by the Institutional Review Board of Wuxi Mental Health Center (approval no. WXMHCIRB2020LLky013; July 29, 2020) and prospectively registered with the Chinese Clinical Trial Registry (ChiCTR2000041231; December 22, 2020). Written informed consent was obtained from all participants.

Consent for publication

Not applicable.

Competing interests

The authors declare that they have no competing interests.

References

1. Winstein CJ, Stein J, Arena R, Bates B, Cherney LR, Cramer SC et al (2016) Guidelines for Adult Stroke Rehabilitation and Recovery: A Guideline for Healthcare Professionals From the American Heart Association/American Stroke Association. Stroke 47:e98–169. https://doi.org/10.1161/STR.0000000000000098
2. Takakusaki K (2017) Functional Neuroanatomy for Posture and Gait Control. J Mov Disord 10:1–17. https://doi.org/10.14802/jmd.16062
3. Binder E, Leimbach M, Pool E-M, Volz LJ, Eickhoff SB, Fink GR et al (2021) Cortical reorganization after motor stroke: A pilot study on differences between the upper and lower limbs. Hum Brain Mapp 42:1013–1033. https://doi.org/10.1002/hbm.25275
4. Vinehout K, Schmit BD, Schindler-Ivens S (2019) Lower Limb Task-Based Functional Connectivity Is Altered in Stroke. Brain Connect 9:365–377. https://doi.org/10.1089/brain.2018.0640
5. Lefaucheur J-P, Aleman A, Baeken C, Benninger DH, Brunelin J, Di Lazzaro V et al (2020) Evidence-based guidelines on the therapeutic use of repetitive transcranial magnetic stimulation (rTMS): An update (2014–2018). Clin Neurophysiol 131:474–528. https://doi.org/10.1016/j.clinph.2019.11.002
6. Tung Y-C, Lai C-H, Liao C-D, Huang S-W, Liou T-H, Chen H-C (2019) Repetitive transcranial magnetic stimulation of lower limb motor function in patients with stroke: a systematic review and meta-analysis of randomized controlled trials. Clin Rehabil 33:1102–1112. https://doi.org/10.1177/0269215519835889
7. Veldema J, Gharabaghi A (2022) Non-invasive brain stimulation for improving gait, balance, and lower limbs motor function in stroke. J Neuroeng Rehabil 19:84. https://doi.org/10.1186/s12984-022-01062-y
8. Deng Z-D, Lisanby SH, Peterchev AV (2013) Electric field depth–focality tradeoff in transcranial magnetic stimulation: Simulation comparison of 50 coil designs. Brain Stimulat 6:1–13. https://doi.org/10.1016/j.brs.2012.02.005
9. Kakuda W, Abo M, Nakayama Y, Kiyama A, Yoshida H (2013) High-frequency rTMS using a double cone coil for gait disturbance. Acta Neurol Scand 128:100–106. https://doi.org/10.1111/ane.12085
10. Huang G, Wang H, Zhao W, Yang J, Zheng Z, Yao W et al (2025) Effects of 10-Hz rTMS over the leg motor cortex using a double-cone coil on lower limb motor recovery in subacute stroke: a randomised, double-blind, sham-controlled study. J Neuroeng Rehabil 22:201. https://doi.org/10.1186/s12984-025-01745-2
11. Luft AR, Macko RF, Forrester LW, Villagra F, Ivey F, Sorkin JD et al (2008) Treadmill exercise activates subcortical neural networks and improves walking after stroke: a randomized controlled trial. Stroke 39:3341–3350. https://doi.org/10.1161/strokeaha.108.527531
12. Enzinger C, Dawes H, Johansen-Berg H (2009) Brain activity changes associated with treadmill training after stroke. Stroke 40:2460–2467. https://doi.org/10.1161/STROKEAHA.109.550053
13. Cui W, Huang L, Tian Y, Luo H, Chen S, Yang Y et al (2022) Effect and mechanism of mirror therapy on lower limb rehabilitation after ischemic stroke: A fMRI study. NeuroRehabilitation 51:65–77. https://doi.org/10.3233/NRE-210307
14. Tang Z, Zhao Y, Sun X, Liu Y, Su W, Liu T et al (2024) Evidence that robot-assisted gait training modulates neuroplasticity after stroke: An fMRI pilot study based on graph theory analysis. Brain Res 1842:149113. https://doi.org/10.1016/j.brainres.2024.149113
15. Hong W, Liu Z, Zhang X, Li M, Yu Z, Wang Y et al (2024) Distance-related functional reorganization predicts motor outcome in stroke patients. BMC Med 22:247. https://doi.org/10.1186/s12916-024-03435-7

16. Peng X, Srivastava S, Sutton F, Zhang Y, Badran BW, Kautz SA (2024) Compensatory increase in ipsilesional supplementary motor area and premotor connectivity is associated with greater gait impairments: a personalized fMRI analysis in chronic stroke. Front Hum Neurosci 18:1340374. https://doi.org/10.3389/fnhum.2024.1340374
17. Pundik S, Skelly MM, McCabe JP, Salameh AI, Anderson T, Duncan KR et al (2025) Resting-State Functional Connectivity of Sensorimotor and Default Mode Networks and Lower Limb Performance in Chronic Stroke: A Cross-Sectional Study. Brain Behav 15:e70519. https://doi.org/10.1002/brb3.70519
18. Koch G, Bonnì S, Casula EP, Iosa M, Paolucci S, Pellicciari MC et al (2019) Effect of cerebellar stimulation on gait and balance recovery in patients with hemiparetic stroke: A randomized clinical trial. JAMA Neurol 76:170–178. https://doi.org/10.1001/jamaneurol.2018.3639
19. Huang G, Zhao Z, Wang D, Bian L, Zheng K, Lu X et al (2026) Cerebellar Functional Reorganization after Intermittent Theta Burst Stimulation over Vermis on Balance Recovery in Subacute Stroke Patients. Brain Stimulat 19:103055. https://doi.org/10.1016/j.brs.2026.103055
20. Richard A, Van Hamme A, Drevelle X, Golmard J-L, Meunier S, Welter M-L (2017) Contribution of the supplementary motor area and the cerebellum to the anticipatory postural adjustments and execution phases of human gait initiation. Neuroscience 358:181–189. https://doi.org/10.1016/j.neuroscience.2017.06.047
21. Akkal D, Dum RP, Strick PL (2007) Supplementary Motor Area and Presupplementary Motor Area: Targets of Basal Ganglia and Cerebellar Output. J Neurosci 27:10659–10673. https://doi.org/10.1523/jneurosci.3134-07.2007
22. Fox M, Raichle M (2007) Spontaneous fluctuations in brain activity observed with functional magnetic resonance imaging. Nat Rev Neurosci 8:700–711. https://doi.org/10.1038/nrn2201
23. Park C, Chang WH, Ohn SH, Kim ST, Bang OY, Pascual-Leone A et al (2011) Longitudinal changes of resting-state functional connectivity during motor recovery after stroke. Stroke 42:1357–1362. https://doi.org/10.1161/STROKEAHA.110.596155
24. Zou Q-H, Zhu C-Z, Yang Y, Zuo X-N, Long X-Y, Cao Q-J et al (2008) An improved approach to detection of amplitude of low-frequency fluctuation (ALFF) for resting-state fMRI: fractional ALFF. J Neurosci Methods 172:137–141. https://doi.org/10.1016/j.jneumeth.2008.04.012
25. Biswal B, Yetkin F, Haughton V, Hyde J (1995) Functional connectivity in the motor cortex of resting human brain using echo-planar MRI. Magn Reson Med 34:537–541. https://doi.org/10.1002/mrm.1910340409
26. Hutchison RM, Womelsdorf T, Allen EA, Bandettini PA, Calhoun VD, Corbetta M et al (2013) Dynamic functional connectivity: Promise, issues, and interpretations. NeuroImage 80:360–378. https://doi.org/10.1016/j.neuroimage.2013.05.079
27. Bonkhoff AK, Rehme AK, Hensel L, Tscherpel C, Volz LJ, Espinoza FA et al (2021) Dynamic connectivity predicts acute motor impairment and recovery post-stroke. Brain Commun 3:fcab227. https://doi.org/10.1093/braincomms/fcab227
28. Folstein MF, Folstein SE, McHugh PR (1975) Mini-mental state. A practical method for grading the cognitive state of patients for the clinician. J Psychiatr Res 12:189. https://doi.org/10.1016/0022-3956(75)90026-6
29. Rossi S, Antal A, Bestmann S, Bikson M, Brewer C, Brockmöller J et al (2021) Safety and recommendations for TMS use in healthy subjects and patient populations, with updates on training, ethical and regulatory issues: Expert Guidelines. Clin Neurophysiol Off J Int Fed Clin Neurophysiol 132:269–306. https://doi.org/10.1016/j.clinph.2020.10.003

30. Rossini PM, Burke D, Chen R, Cohen LG, Daskalakis Z, Di Iorio R et al (2015) Non-invasive electrical and magnetic stimulation of the brain, spinal cord, roots and peripheral nerves: Basic principles and procedures for routine clinical and research application. An updated report from an I.F.C.N. Committee. Clin Neurophysiol Off J Int Fed Clin Neurophysiol 126:1071. https://doi.org/10.1016/j.clinph.2015.02.001
31. Fugl-Meyer A, Jääskö L, Leyman I, Olsson S, Steglind S (1975) The post-stroke hemiplegic patient. 1. a method for evaluation of physical performance. J Rehabil Med 7:13–31. https://doi.org/10.2340/1650197771331
32. Gladstone D, Danells C, Black S (2002) The fugl-meyer assessment of motor recovery after stroke: a critical review of its measurement properties. Neurorehabil Neural Repair 16:232–240. https://doi.org/10.1177/154596802401105171
33. Yan C-G, Wang X-D, Zuo X-N, Zang Y-F (2016) Data Processing & Analysis for (Resting-State). Brain Imaging Neuroinformatics 14:339–351. https://doi.org/10.1007/s12021-016-9299-4
34. Yan C-G, Zang Y-FDPARSF (2010) Front Syst Neurosci 4:13. https://doi.org/10.3389/fnsys.2010.00013. A MATLAB Toolbox for Pipeline Data Analysis of Resting-State fMRI
35. Song X-W, Dong Z-Y, Long X-Y, Li S-F, Zuo X-N, Zhu C-Z et al (2011) REST: a toolkit for resting-state functional magnetic resonance imaging data processing. PLoS ONE 6:e25031. https://doi.org/10.1371/journal.pone.0025031
36. Mayka MA, Corcos DM, Leurgans SE, Vaillancourt DE (2006) Three-dimensional locations and boundaries of motor and premotor cortices as defined by functional brain imaging: a meta-analysis. NeuroImage 31:1453–1474. https://doi.org/10.1016/j.neuroimage.2006.02.004
37. Prodoehl J, Yu H, Little DM, Abraham I, Vaillancourt DE (2008) Region of interest template for the human basal ganglia: comparing EPI and standardized space approaches. NeuroImage 39:956–965. https://doi.org/10.1016/j.neuroimage.2007.09.027
38. Rolls ET, Huang C-C, Lin C-P, Feng J, Joliot M (2020) Automated anatomical labelling atlas 3. NeuroImage 206:116189. https://doi.org/10.1016/j.neuroimage.2019.116189
39. Leonardi N, Van De Ville D (2015) On spurious and real fluctuations of dynamic functional connectivity during rest. NeuroImage 104:430. https://doi.org/10.1016/j.neuroimage.2014.09.007
40. Hindriks R, Adhikari MH, Murayama Y, Ganzetti M, Mantini D, Logothetis NK et al (2016) Can sliding-window correlations reveal dynamic functional connectivity in resting-state fMRI? NeuroImage. 127:242–256. https://doi.org/10.1016/j.neuroimage.2015.11.055
41. Kriegeskorte N, Simmons WK, Bellgowan PSF, Baker CI (2009) Circular analysis in systems neuroscience: the dangers of double dipping. Nat Neurosci 12:535–540. https://doi.org/10.1038/nn.2303
42. Siebner HR, Funke K, Aberra AS, Antal A, Bestmann S, Chen R et al (2022) Transcranial magnetic stimulation of the brain: What is stimulated? - A consensus and critical position paper. Clin Neurophysiol Off J Int Fed Clin Neurophysiol 140:59–97. https://doi.org/10.1016/j.clinph.2022.04.022
43. Guggisberg AG, Koch PJ, Hummel FC, Buetefisch CM (2019) Brain networks and their relevance for stroke rehabilitation. Clin Neurophysiol Off J Int Fed Clin Neurophysiol 130:1098–1124. https://doi.org/10.1016/j.clinph.2019.04.004
44. Volz LJ, Rehme AK, Michely J, Nettekoven C, Eickhoff SB, Fink GR et al (2016) Shaping Early Reorganization of Neural Networks Promotes Motor Function after Stroke. Cereb Cortex N Y N 1991. 26:2882–2894. https://doi.org/10.1093/cercor/bhw034
45. Du J, Yao W, Li J, Yang F, Hu J, Xu Q et al (2022) Motor Network Reorganization After Repetitive Transcranial Magnetic Stimulation in Early Stroke Patients: A Resting State fMRI Study. Neurorehabil Neural Repair 36:61–

68. https://doi.org/10.1177/15459683211054184
46. Di Pino G, Pellegrino G, Assenza G, Capone F, Ferreri F, Formica D et al (2014) Modulation of brain plasticity in stroke: a novel model for neurorehabilitation. Nat Rev Neurol 10:597–608. https://doi.org/10.1038/nrneurol.2014.162
47. Xu J, Branscheidt M, Schambra H, Steiner L, Widmer M, Diedrichsen J et al (2019) Rethinking interhemispheric imbalance as a target for stroke neurorehabilitation. Ann Neurol 85:502–513. https://doi.org/10.1002/ana.25452
48. Bestmann S, Swayne O, Blankenburg F, Ruff CC, Teo J, Weiskopf N et al (2010) The role of contralesional dorsal premotor cortex after stroke as studied with concurrent TMS-fMRI. J Neurosci Off J Soc Neurosci 30:11926–11937. https://doi.org/10.1523/jneurosci.5642-09.2010
49. Hensel L, Bonkhoff AK, Paul T, Tscherpel C, Lange F, Viswanathan S et al (2025) The role of contralesional regions for post-stroke movements revealed by dynamic connectivity and TMS interference. NeuroImage Clin 47:103825. https://doi.org/10.1016/j.nicl.2025.103825
50. Wang H, Xiong X, Zhang K, Wang X, Sun C, Zhu B et al (2023) Motor network reorganization after motor imagery training in stroke patients with moderate to severe upper limb impairment. CNS Neurosci Ther. https://doi.org/10.1111/cns.14065
51. Zhang K, Ding L, Wang X, Zhuang J, Tong S, Jia J et al (2024) Evidence of mirror therapy for recruitment of ipsilateral motor pathways in stroke recovery: A resting fMRI study. Neurother J Am Soc Exp Neurother 21:e00320. https://doi.org/10.1016/j.neurot.2024.e00320
52. Bostan A, Strick P (2018) The basal ganglia and the cerebellum: nodes in an integrated network. Nat Rev Neurosci 19:338–350. https://doi.org/10.1038/s41583-018-0002-7
53. Buckner RL, Krienen FM, Castellanos A, Diaz JC, Yeo BTT (2011) The organization of the human cerebellum estimated by intrinsic functional connectivity. J Neurophysiol 106:2322–2345. https://doi.org/10.1152/jn.00339.2011
54. King M, Hernandez-Castillo CR, Poldrack RA, Ivry RB, Diedrichsen J (2019) Functional boundaries in the human cerebellum revealed by a multi-domain task battery. Nat Neurosci 22:1371–1378. https://doi.org/10.1038/s41593-019-0436-x
55. Guell X, Schmahmann J (2020) Cerebellar Functional Anatomy: a Didactic Summary Based on Human fMRI Evidence. Cerebellum Lond Engl 19:1–5. https://doi.org/10.1007/s12311-019-01083-9
56. Spampinato DA, Block HJ, Celnik PA (2017) Cerebellar-M1 Connectivity Changes Associated with Motor Learning Are Somatotopic Specific. J Neurosci Off J Soc Neurosci 37:2377–2386. https://doi.org/10.1523/jneurosci.2511-16.2017
57. Liu G, Guo Y, Dang C, Peng K, Tan S, Xie C et al (2021) Longitudinal changes in the inferior cerebellar peduncle and lower limb motor recovery following subcortical infarction. BMC Neurol 21:320. https://doi.org/10.1186/s12883-021-02346-x
58. Delion T, Jacquemont T, Daghsen L, Valabregue R, Beanato E, Hummel F et al (2025) Resting-State Cortico-Cerebellar Connectivity Correlates with Post-Stroke Motor Recovery - A Prospective Functional MRI Study. Cerebellum Lond Engl 24:28. https://doi.org/10.1007/s12311-024-01783-x
59. Lu R, Pang Z, Gao T, He Z, Hu Y, Zhuang J et al (2025) Multisensory BCI promotes motor recovery via high-order network-mediated interhemispheric integration in chronic stroke. BMC Med 23:380. https://doi.org/10.1186/s12916-025-04214-8

60. Zhao L, Chen L, Wang C, Li S, Wan C (2024) Effects of repetitive transcranial magnetic stimulation at different targets on brain function in stroke patients: a randomized controlled trial. Front Neurol 15:1454220. https://doi.org/10.3389/fneur.2024.1454220
61. MacKinnon DP, Krull JL, Lockwood CM (2000) Equivalence of the Mediation, Confounding and Suppression Effect. Prev Sci 1:173–181. https://doi.org/10.1023/a:1026595011371
62. Yu H, Wang H, Liu S, Jing J, Huang G, Zhang Y et al (2026) Post-task resting-state fMRI of walking-related neural activity in patients with stroke: immediate and delayed brain network dynamics. Ann Med 58:2662817. https://doi.org/10.1080/07853890.2026.2662817
63. Allen EA, Damaraju E, Plis SM, Erhardt EB, Eichele T, Calhoun VD (2014) Tracking whole-brain connectivity dynamics in the resting state. Cereb Cortex N Y N 1991. 24:663–676. https://doi.org/10.1093/cercor/bhs352
64. Preti MG, Bolton TA, Van De Ville D (2017) The dynamic functional connectome: State-of-the-art and perspectives. NeuroImage 160:41–54. https://doi.org/10.1016/j.neuroimage.2016.12.061
65. Qin Y, Liu X, Guo X, Liu M, Li H, Xu S (2021) Low-Frequency Repetitive Transcranial Magnetic Stimulation Restores Dynamic Functional Connectivity in Subcortical Stroke. Front Neurol 12:771034. https://doi.org/10.3389/fneur.2021.771034
66. Lurie DJ, Kessler D, Bassett DS, Betzel RF, Breakspear M, Kheilholz S et al (2020) Questions and controversies in the study of time-varying functional connectivity in resting fMRI. Netw Neurosci Camb Mass 4:30–69. https://doi.org/10.1162/netn_a_00116
67. Laumann TO, Snyder AZ, Gratton C (2024) Challenges in the measurement and interpretation of dynamic functional connectivity. Imaging Neurosci Camb Mass 2:imag–2. https://doi.org/10.1162/imag_a_00366
68. Power JD, Barnes KA, Snyder AZ, Schlaggar BL, Petersen SE (2012) Spurious but systematic correlations in functional connectivity MRI networks arise from subject motion. NeuroImage 59:2142–2154. https://doi.org/10.1016/j.neuroimage.2011.10.018
69. Ciric R, Wolf DH, Power JD, Roalf DR, Baum GL, Ruparel K et al (2017) Benchmarking of participant-level confound regression strategies for the control of motion artifact in studies of functional connectivity. NeuroImage 154:174. https://doi.org/10.1016/j.neuroimage.2017.03.020
70. Siegel JS, Snyder AZ, Ramsey L, Shulman GL, Corbetta M (2016) The effects of hemodynamic lag on functional connectivity and behavior after stroke. J Cereb Blood Flow Metab 36:2162–2176. https://doi.org/10.1177/0271678x15614846

Figures

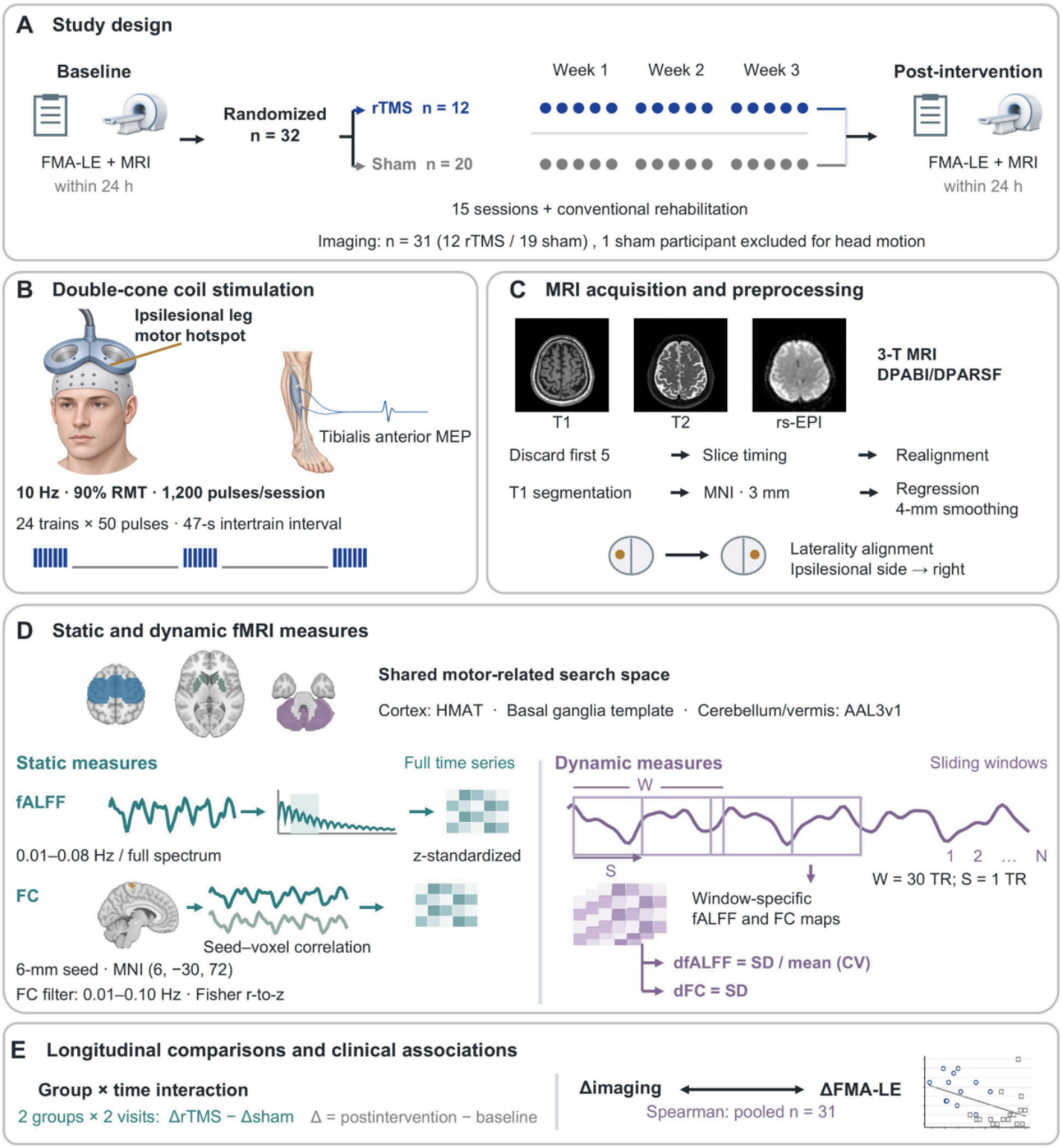


Figure 1

Study design and resting-state fMRI analysis framework. A, Baseline and postintervention assessments, with 15 sessions of rTMS or sham stimulation over 3 weeks alongside conventional rehabilitation. B, Double-cone coil stimulation targeted the ipsilesional leg motor hotspot, localized using tibialis anterior motor-evoked potentials or the mirrored contralesional hotspot when ipsilesional responses were absent. C, MRI acquisition, preprocessing, and image alignment with the ipsilesional hemisphere on the right. D, Static fALFF and seed-based FC were calculated across the full time series; dynamic measures quantified their variability across sliding windows within the same

motor-related search space. Both static and window-specific fALFF used the 0.01–0.08-Hz band. Dynamic analyses used a 30-TR Hamming window (W) advanced in 1-TR steps (S). dFALFF was expressed as the coefficient of variation (CV = SD/mean), and dFC as the standard deviation (SD). E, Group × time comparisons and Spearman correlations between imaging changes and FMA-LE improvement in the pooled sample (n = 31). Δ, postintervention minus baseline; TR, repetition time. Device and signal illustrations are schematic.

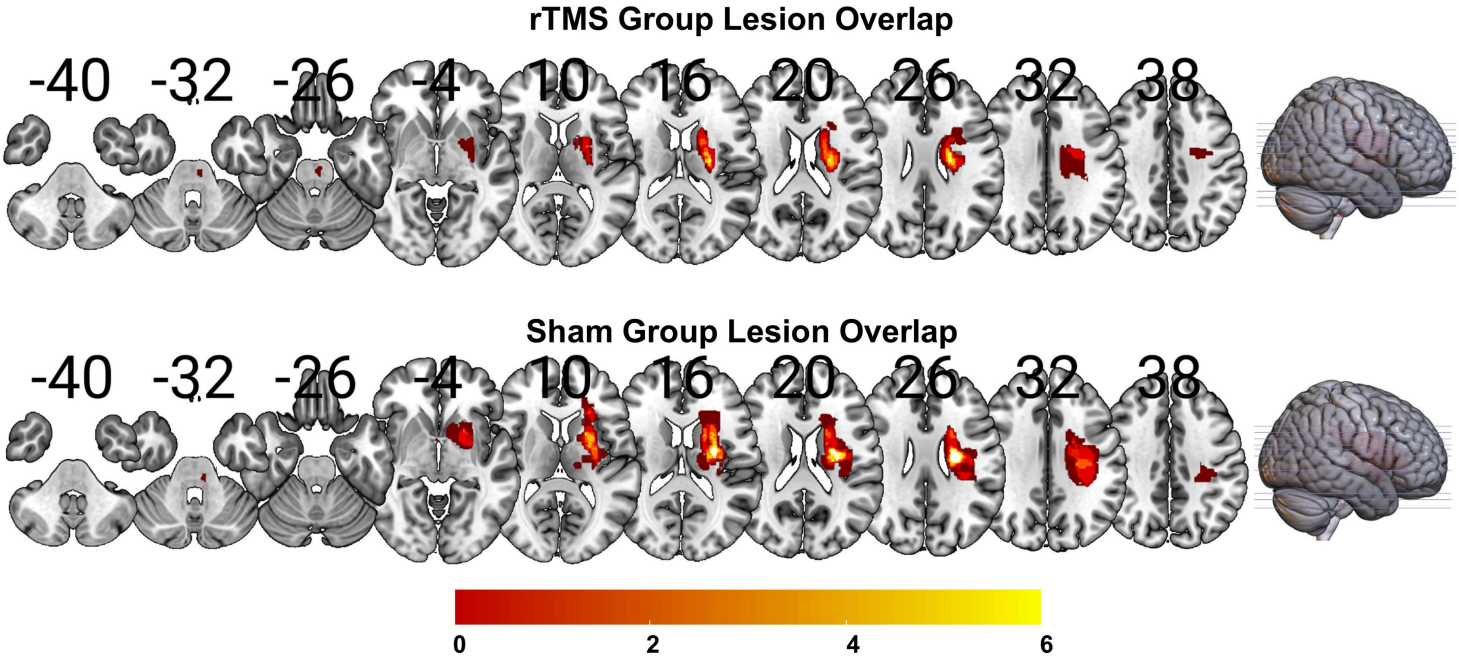


Figure 2

Lesion overlap maps in the rTMS and sham groups. The upper and lower rows show the rTMS and sham groups, respectively. Left-sided lesions were flipped to the right hemisphere for visualization. Colors indicate the number of participants with overlapping lesions at each voxel. Slice labels denote MNI z coordinates (mm); lateral brain views indicate slice locations.

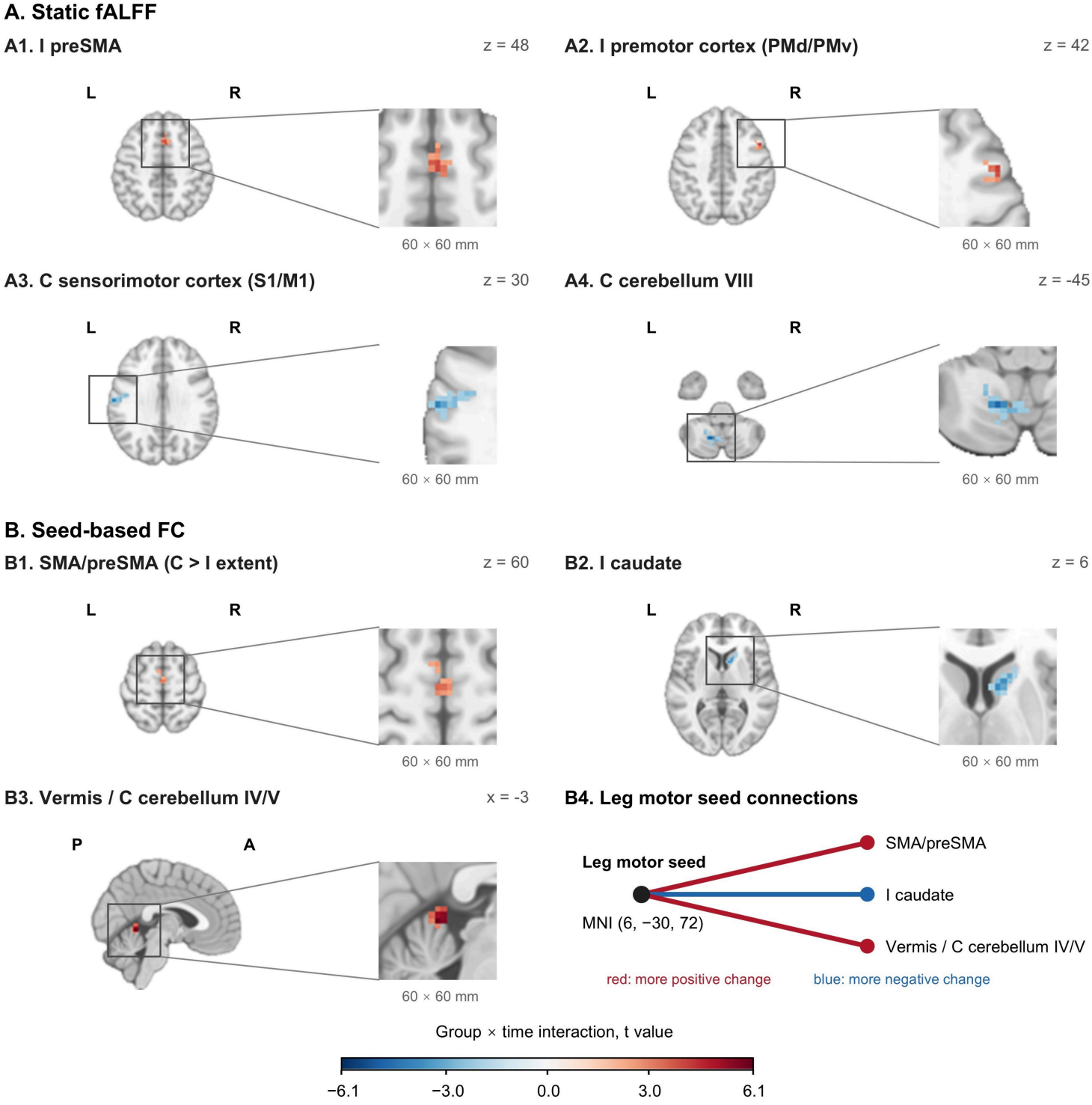


Figure 3

Group-by-time effects on static fALFF and functional connectivity. A1–A4, fALFF effects in predominantly ipsilesional preSMA, ipsilesional premotor cortex, contralesional sensorimotor cortex, and contralesional cerebellar lobule VIII. **B1–B3**, FC effects between the leg motor seed and SMA/preSMA, ipsilesional caudate, and vermis/contralesional cerebellar lobules IV/V. The SMA/preSMA region extends bilaterally, predominantly contralesionally. **B4**, Schematic summary of these connections. Red and blue indicate more positive and more negative changes in rTMS relative to sham, respectively; brain-map colors represent interaction t values. Boxes mark the corresponding 60 × 60-mm enlarged views. Coordinates are in MNI space (mm). I/C, ipsilesional/contralesional;

SMA/preSMA, supplementary/pre-supplementary motor area; PMd/PMv, dorsal/ventral premotor cortex; S1/M1, primary somatosensory/motor cortex; L/R, left/right; A/P, anterior/posterior.

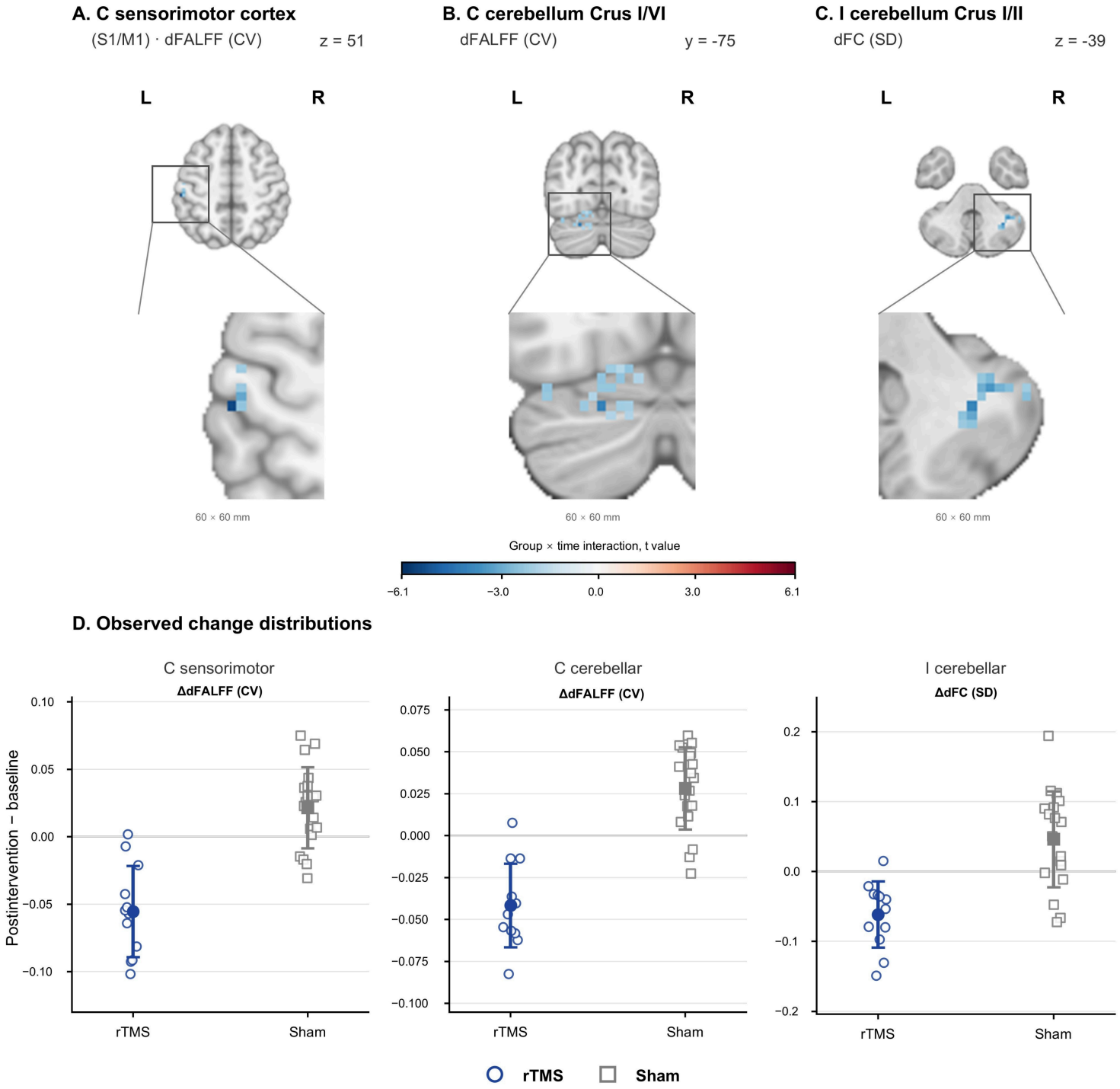


Figure 4

Group-by-time effects on dynamic fALFF and functional connectivity. A–B, dFALFF coefficient of variation (CV). **C**, dFC standard deviation (SD). Brain-map colors represent interaction t values for (rTMS post − pre) − (sham post − pre). Boxes mark 60 × 60-mm enlarged views; coordinates are in MNI space (mm). **D**, Individual changes (postintervention − baseline) and group mean ± SD. Open symbols represent participants; filled symbols and error bars indicate means and SDs. Blue circles denote rTMS (n = 12), and gray squares sham (n = 19). Descriptive

between-group comparisons of change scores are provided in Supplementary Table S4. C/I, contralesional/ipsilesional; L/R, left/right; S1/M1, primary somatosensory/motor cortex.

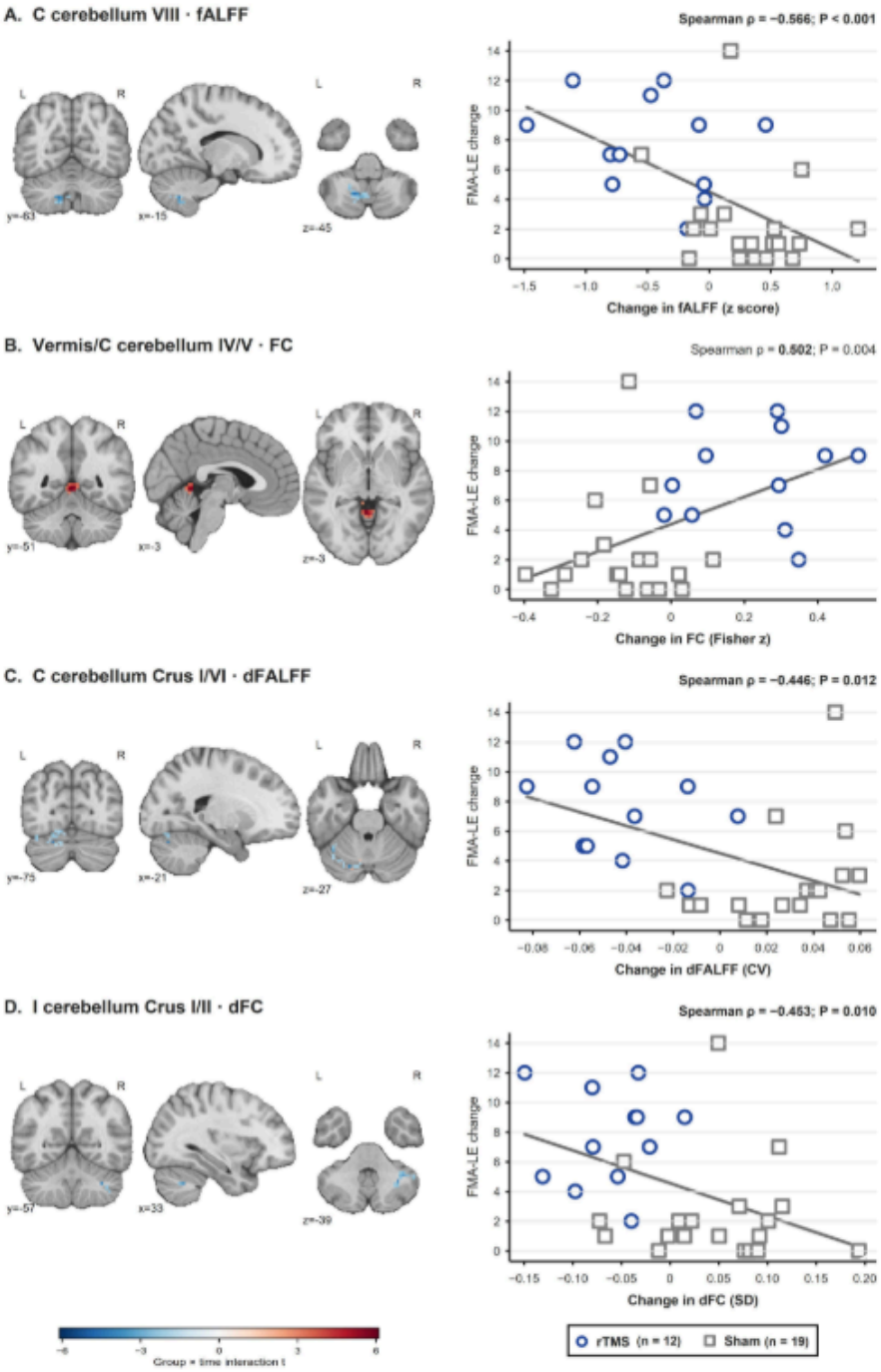


Figure 5

Associations between cerebellar imaging changes and motor improvement. A–D, fALFF, FC, dFALFF, and dFC changes versus FMA-LE improvement. Changes are postintervention minus baseline. Annotations report pooled Spearman correlations (n = 31) and two-sided, unadjusted P values; gray lines show pooled ordinary least-squares fits for visualization. Brain maps display group-by-time interaction t values. Coordinates are in MNI space (mm). CV, coefficient of variation; SD, standard deviation; C/I, contralesional/ipsilesional; L/R, left/right in lesion-aligned images.

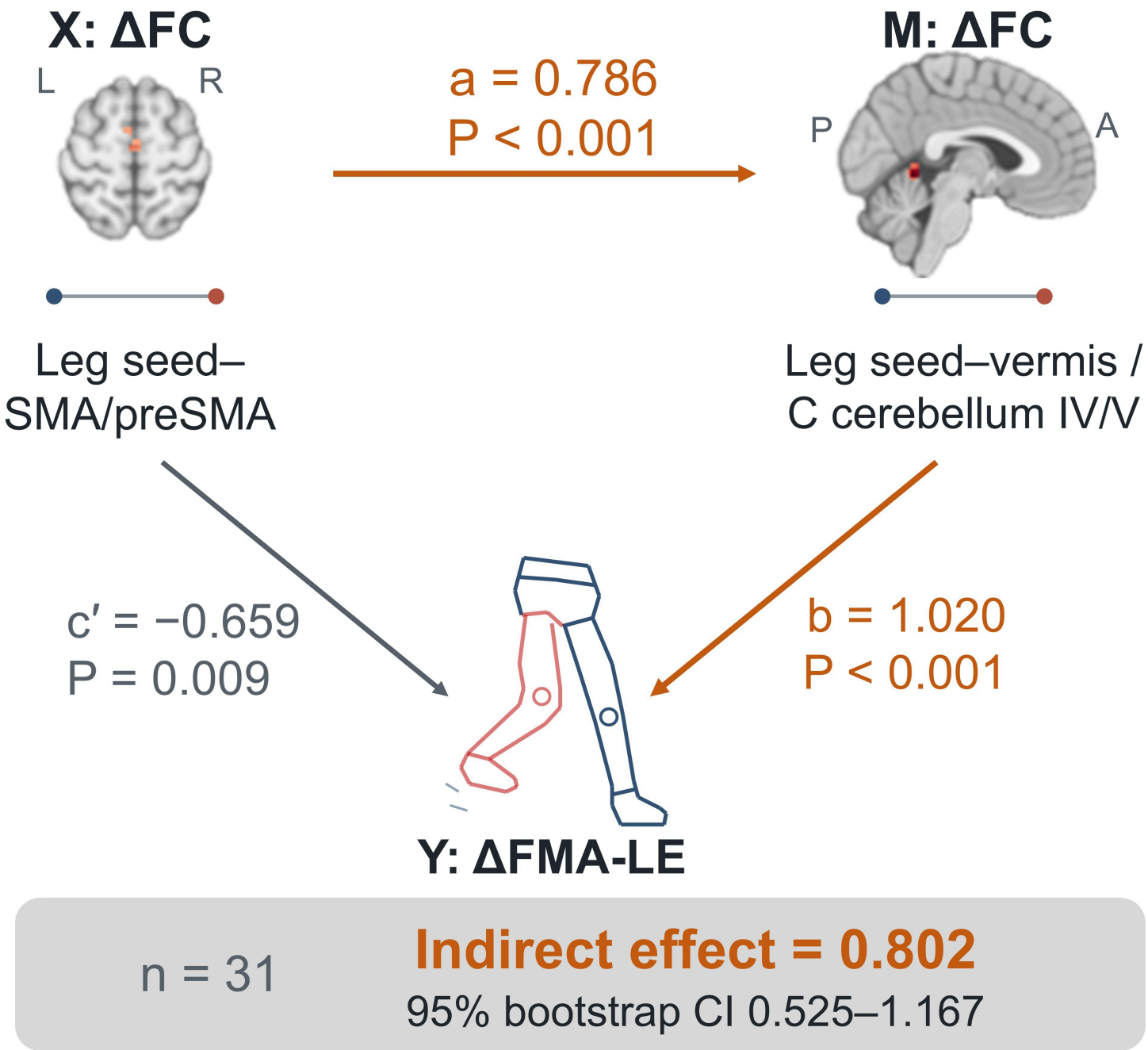


Figure 6

Exploratory indirect associations between connectivity changes and motor improvement. X and M denote leg motor seed connectivity changes with SMA/preSMA and vermis/contralesional cerebellar IV/V, respectively; Y denotes FMA-LE improvement. Arrows show standardized coefficients: a, X→M; b, M→Y adjusted for X; c', X→Y adjusted for M. Orange and gray indicate positive and negative coefficients. The indirect effect (a×b) has a nominal 95% confidence interval from 20,000 group-stratified bootstrap resamples. P values are two-sided; Full path estimates are provided in Supplementary Table S7. Δ, postintervention minus baseline; C, contralesional; L/R, left/right; A/P, anterior/posterior.